

Resonant heating of Fe₃O₄ and hemozoin nanoparticles dispersed in D₂O by RF excitation of transitions between Zeeman components

I.V. Khmelinskii^a, V.I. Makarov^{b,*}

^a Universidade do Algarve, FCT, DQF and CIQA, 8005-139 Faro, Portugal

^b Department of Physics, University of Puerto Rico, Rio Piedras, PO Box 23343, San Juan, PR 00931-3343, USA

ARTICLE INFO

Article history:

Received 18 October 2017

In final form 15 March 2018

Available online 17 March 2018

ABSTRACT

Presently we evaluated the natural relaxation frequency of the spin angular momentum of Fe₃O₄ and hemozoin superparamagnetic (SP) nanoparticles in D₂O solutions in function of the sample temperature. The sample was composed of 1% H₂O in D₂O with dispersed Fe₃O₄ or hemozoin nanoparticles at variable number density. The natural relaxation frequencies are in the sub-MHz and MHz range for the Fe₃O₄ and hemozoin nanoparticles, respectively. We studied resonance heating of the same samples. We found that scanning the external magnetic field strength in a constant-frequency radio-frequency (RF) electromagnetic field, with its magnetic field component perpendicular to the external magnetic field, we obtain resonant heating at the magnetic field strength of 50 or 100 Gs for the RF excitation at 150 or 300 MHz, respectively. The measured resonance line has a Lorentzian form, with the heating amplitude dependent on the number density of SP nanoparticles, RF power and time. The resonance width correlates with the natural relaxation frequency of the spin angular momentum of the SP nanoparticles. We describe a theoretical model explaining the experimental results. As the achievable heating rate is directly proportional to the spin relaxation rate of the SP nanoparticles, we expect two orders of magnitude higher heating rates in suspensions based on water with natural isotopic composition.

Published by Elsevier B.V.

1. Introduction

Superparamagnetic nanostructured materials are receiving a lot of scrutiny due to their unique properties and potential applications. The SP nanoparticles may be used in a range of biomedical applications including hyperthermia, imaging and drug delivery. The ability to locally generate heat in response to an oscillating magnetic field makes such particles ideal for these purposes [1,2]. SP nanoparticles may be used in diagnostics [3], magnetic separation [4,5], as contrast agents in MRI [6,7], thermo responsive drug carriers [8], and in hyperthermia [9,10]. The latter is a promising approach that may be used to induce thermally activated therapy of a tumor [10,11]. The technical problem in hyperthermia is local heating of the tumor area without damaging much of the surrounding healthy cells. Therefore, it is important that SP nanoparticles would accumulate in the tumor area only. It was, however, proposed that SP nanoparticles may be conveniently transported to the location of the tumor tissue by interventional techniques

[11]. As we noted earlier [12], SP nanoparticles of ferrites (such as magnetite Fe₃O₄) and hemozoin are good candidates for hyperthermal applications, as both have excellent high-frequency response and high electric resistivity. We therefore expect that both these nanostructures will have high magnetic losses and consequently high heating ability.

The hyperthermic effect of Fe₃O₄ SP nanoparticles was tested for treatment of different tumors. The RF electromagnetic field was used as an energy source to activate thermally responsive nanoparticles, providing for controlled local drug delivery to cancer cells [13]. Namely, 180 ± 20 nm sized chitosan-graft-poly(*N*-vinyl caprolactam) nanoparticles containing Fe₃O₄ nanoparticles were selectively delivered into the breast cancer cells in vivo [13]. The initial results [13] strongly support future development of RF-assisted drug delivery by nanoparticles, for improved tumor targeting in breast cancer treatment. Micrometer-sized Fe₃O₄ powders, chemically prepared and processed in RF (13.56 MHz) oxygen plasma, were used to produce biocompatible ferro-fluids down to nanoscopic size for biomaterial applications [14]. Hyperthermia induced by ferromagnetic resonance in nanostructured Fe and Fe₃O₄ was also explored [15]. Biocompatible luminescent and photoactive SP nanocomposites were synthesized with Fe₃O₄/SiO₂ and

Abbreviations: SP, superparamagnetic; RF, radio-frequency.

* Corresponding author at: Department of Physics, University of Puerto Rico, Rio Piedras Campus, PO Box 23343, San Juan, PR 00931-3343, USA.

E-mail address: vladimir.makarov@upr.edu (V.I. Makarov).

$\text{Fe}_3\text{O}_4/\text{TiO}_2$ composition [16–18], with good potential for applications involving in vivo nanohyperthermia and cancer treatment.

Thus, quite a few reports addressed the SP Fe_3O_4 nanoparticles, with little attention devoted to SP hemozoin, generated by malaria parasites. Note that selective RF heating of such nanocrystals may be used as malaria treatment, by destroying the parasite. We reported that hemozoin nanoparticles have SP properties, measuring natural electron spin relaxation rates for both Fe_3O_4 and hemozoin nanoparticles in liquid CS_2 [12,19]. Presently we use the previously developed approach [12] to measure the natural spin relaxation parameters for both Fe_3O_4 and hemozoin in aqueous solutions, important for biomedical applications. This approach involves evaluation of broadening of the ^1H NMR line of H_2O induced by SP nanoparticles dispersed in D_2O . Taking into account the evaluated spin relaxation parameters, we studied resonance RF heating (100–500 MHz range) for both Fe_3O_4 and hemozoin nanoparticles dispersed in D_2O with 1% H_2O . We report large resonance heating effect, as compared to usually modest conventional RF heating, and provide detailed theoretical analysis of the results obtained. The presently reported results are novel and demonstrate high feasibility of the future biomedical applications in resonant hyperthermia treatment of malaria and cancer.

2. Experimental setup

2.1. Equipment and measurements

Detailed characterization and description of the nanostructured Fe_3O_4 and hemozoin powders and the NMR experimental techniques were reported earlier [12] and will not be presented here in detail. Fig. 1 shows the block diagram for the RF heating experiments.

As shown in Fig. 1a, a Pyrex NMR tube (4) was placed between two rectangular brass electrodes ($5 \times 10 \text{ mm}^2$), with the gap between them variable by a stepper motor, controlled in the Lab-View environment running on a PC. Two magnetic field coils ($D_I = 5 \text{ cm}$; $D_E = 7 \text{ cm}$; $L = 1 \text{ cm}$), wound in 2 mm copper wire, were installed coaxially normal to the NMR tube, creating magnetic

fields up to 350 Gs. The sample temperature was monitored by an IR camera (Aerial Thermography with Optris PI LightWeight; Optics Technical Data Inc.). The camera looked through the opening in one of the coils, with its objective lens 6 cm away from the coil. The magnetic field was homogeneous within 1% in the sample volume. An RF source (High Power Signal Generator APSIN26G-TP, ANI PICO Inc. Switzerland) was connected to the brass electrodes by a 50Ω coaxial cable 1.0 m long. A fraction of the RF signal was sent to a digital oscilloscope (LeCroy Wavesurfer 62XS Digital Storage Oscilloscope 600 MHz) to control the signal frequency and amplitude. The sample tube was installed reproducibly into the setup.

In the modified experimental setup, the RF source was disconnected from the electrodes (1) and connected to a pair of solenoids as shown in Fig. 1b. Each solenoid was wound with copper wire 2 mm in diameter, making a coil 6 mm i. d. The two solenoids were connected in series, creating a magnetic field along the z axis of the reference system, coinciding with the common axis of the two solenoids and with the sample tube axis. The two solenoids were mounted to create a 1 cm gap between them. This modified setup was used to compare the resonance heating effect induced by electric and magnetic excitation.

2.2. Sample preparation

Commercial hemozoin (InvivoGen, France; 93–95%; average nanocrystal size $17.5 \times 3.1 \times 3.1 \text{ nm}^3$) and Fe_3O_4 (MTI Corporation; special order: average size $3.7 \pm 1.5 \text{ nm}$) were used as obtained. The presently used hemozoin powder was characterized earlier [12]. The samples were prepared as follows: 1 ml bidistilled deionized H_2O was dissolved in 99 ml high purity D_2O (Sigma-Aldrich); 1 ml of the solvent mixture was transferred into a 1.5 ml glass vial; 6 mg of commercial hemozoin was placed into the vial; the mixture was ultrasonicated for 20 min; 0.2 ml of the sample was transferred into an NMR tube; 0.2 ml of the solvent mixture was added to the remaining suspension (0.8 ml). The last two steps were repeated 8 more times, preparing the total of 9 progressively diluted suspension samples, with an additional control sample containing the solvent mixture only. The Fe_3O_4 samples were prepared in the same way.

The number densities of hemozoin and Fe_3O_4 nanocrystals in the most concentrated suspensions were estimated earlier [12]: $3.75 \times 10^{10} \text{ cm}^{-3}$ and $5.47 \times 10^{13} \text{ cm}^{-3}$, respectively.

2.3. NMR measurements

NMR spectra were recorded on a Bruker FOURIER-300 MHz NMR spectrometer equipped with a 16-position SampleXpress Lite sample changer: 5 mm DUL EasyProbe ^1H and ^{13}C , with z-PFG, operating with TOPSPIN 3.1 software under Windows 7 Professional. The sample temperature could be set between -30°C and 120°C , using the ER 4131VT temperature control system (Bruker Inc.). Digital signal recording provided for averaging the signal over multiple measurement cycles.

2.4. Measurements of the resonant RF heating

At a given frequency the gap between the electrodes was adjusted to maximize the RF absorption by the sample, by minimizing the amplitude of the signal recorded by the oscilloscope, with the resulting gap maintained constant in all measurements performed at that frequency. The heating dynamics and the temperature distribution were monitored by the IR camera connected to the PC. We also explored the heating in function of the SP nanoparticle number density and of the RF power. The tempera-

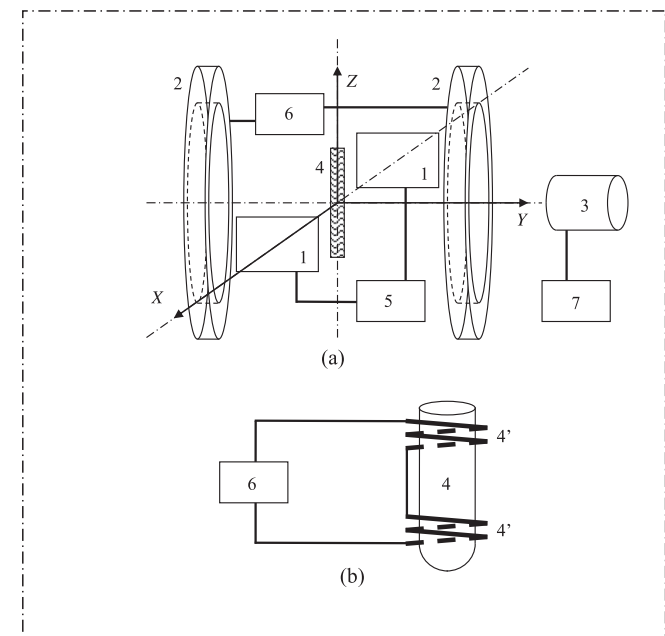


Fig. 1. Block diagram of the experimental setup, (a): (1) RF electrodes; (2) Magnetic field coils; (3) IR camera; (4) Sample; (5) DC source; (6) RF source; (7) Data acquisition system; (b): The RF source was disconnected from the electrodes and connected to the coils; (4') RF coils.

Download English Version:

<https://daneshyari.com/en/article/7837179>

Download Persian Version:

<https://daneshyari.com/article/7837179>

[Daneshyari.com](https://daneshyari.com)